MOLECULAR PHYSICS, 1997, VOL. 92, NO. 4, 651–665

Virial coefficients and equation of state of hard ellipsoids

By CARLOS VEGA
Departamento de Química Física, Facultad de Ciencias Químicas, Universidad Complutense, 28040 Madrid, Spain

(*Received 19 February 1997; revised version accepted 28 April 1997*)

The first five virial coefficients of hard ellipsoids have been evaluated numerically. Hard ellipsoids with length to breadth ratio in the range 3 to 10 were considered. Differences in the virial coefficients between prolate, oblate and biaxial ellipsoids with the same length to breadth ratio have been analysed. We were able to fit the virial coefficient data of hard ellipsoids to an empirical expression which contains only two non-sphericity parameters. This expression describes also correctly the virial coefficient of other convex bodies such as hard spherocylinders. Furthermore, computer simulations were performed for hard ellipsoids. It is found that for a given volume fraction and length to breadth ratio, the compressibility factor of the biaxial ellipsoid is smaller than that of the prolate spheroid, while the compressibility factor of the prolate spheroid is smaller than that of the oblate spheroid. However, differences in the compressibility factor for these three hard models were found to be small. This is surprising since their virial coefficients are quite different. An explanation for this is proposed. The accuracy of several analytical equations of state for hard convex bodies was analysed. Although these equations provide reasonable results they predict the same equation of state for prolate and oblate spheroids. Moreover these equations do not provide good predictions of virial coefficients for very elongated molecules. A new equation of state which uses the computed values of the first five virial coefficients of hard ellipsoids is proposed. This new equation of state is basically a truncated virial expansion, which uses Parsons-like scaling to estimate virial coefficients higher than the fifth. It is shown that this new equation of state performs better than those previously proposed for hard ellipsoids. Moreover it distinguishes between prolate, oblate and biaxial ellipsoids. The new equation of state describes satisfactorily the computer simulation data of hard spherocylinders.

1. Introduction

The study of hard bodies plays an important role within liquid state theory [1, 2]. This is because at high densities, the structure of a fluid is dominated by the repulsive forces. Moreover, phase transitions such as freezing or liquid crystal formation are present in hard bodies [3–5], so that their study may help to understand the origin of these transitions in nature.

In this work we shall focus on hard bodies whose anisotropy is big enough to form a liquid crystal phase. Among the hard models able to form liquid crystal phases, hard ellipsoids of revolution are one of the most popular. Computer simulations of hard ellipsoids were pioneered by Vieillard-Baron [4] in two dimensions, and by Frenkel and Mulder [5] in three dimensions. Frenkel and Mulder found a nematic phase when the ellipsoids of revolution were sufficiently anisotropic [5]. More recently, Rigby has determined the first five virial coefficients of hard ellipsoids of revolution [6]. From the theoretical point of view, a number of theoretical studies on the fluid–nematic transition have been presented [7–11]. However, up to now most of the simulations and theoretical work have focused on hard ellipsoids of revolution. For these models two of the main semiaxes of the ellipsoid have the same length so that the molecule has uniaxial symmetry. Uniaxial hard ellipsoids of revolution are commonly denoted as prolate spheroids, when the third semiaxis is larger than the other two, and oblate spheroids when it is smaller.

In recent years the interest in biaxial hard bodies has increased considerably. Motivation for this is twofold. First, the symmetry of real nematogens is biaxial rather than uniaxial [12]. It is thought that this affects strongly the density jump of the isotropic–nematic transition [12, 13]. Second, biaxial molecules may present biaxial phases in which the molecules are oriented along their principal and secondary axes [14–17]. For these two reasons biaxial hard ellipsoids have received attention lately. The three perpendicular axes of the hard ellipsoids are denoted as a, b and c and they are in general of different length. When two of them are identical, the hard ellipsoid becomes a hard spheroid. Some years ago Allen performed computer simulations of biaxial hard ellipsoids [16], while their phase diagram has been considered in some theoretical studies [13–15].

In this work we focus on hard biaxial ellipsoids.

However, our interest here is on the isotropic phase. Little is known on the effect of biaxiality on the equation of state and virial coefficients of hard particles. This is a matter of interest since in many situations real molecules are modelled as uniaxial, whereas it would probably be a better choice to take a biaxial core. The choice of uniaxial models to describe the shape of real molecules is justified only due to our ignorance of the behaviour of biaxial particles. Another reason to study the isotropic phase of hard ellipsoids is that theories of liquid crystal formation of biaxial models often need a good equation of state for the isotropic phase of the biaxial molecule. In this work the first five virial coefficients of hard ellipsoids will be determined numerically. The second virial coefficient can be obtained exactly by using convex body [18, 19] geometry, but the third, fourth and fifth will be evaluated numerically. The study of virial coefficients is of interest *per se* when dealing with very anisotropic molecules, since the range of the isotropic phase shrinks considerably with increasing molecular anisotropy [3] so that the virial expansion provides a better description of the isotropic phase as the molecular elongation increases. In addition to this we have performed a computer simulation of hard ellipsoids. Our motivation is to analyse the effect of biaxiality on the equation of state. Finally several equations of state proposed for hard convex bodies will be tested. In particular we shall consider the equations of state (EOSs) proposed by Nezbeda [20], Boublík [21], Parsons [22], and Song and Mason [23]. All these equations use only one parameter related to the second virial coefficient, so that they predict the same EOS for prolate and oblate hard spheroids and for hard ellipsoids with the same second virial coefficient. We propose a new EOS for hard ellipsoids which uses the information given by the first five virial coefficients. This new EOS provides better results than those previously proposed and distinguishes prolate, oblate and biaxial hard particles.

2. Calculation details

The hard ellipsoid model presents three principal axes, and the diameter of the molecule along these principal directions is given by $a : b : c$. We shall assume $a < b < c$. We take a as the unit of length and therefore the three diameters of the ellipsoid are $1 : b : c$. Prolate spheroids can be written as $1 : 1 : c$ (the parameter c in this case is commonly denoted in the literature as k), and oblate spheroids as $1 : c : c$. The general case is that of an ellipsoid with $1 : b : c$ with b different from 1 and c.

The second virial coefficient of any hard convex body (hard ellipsoids are a particular case of convex bodies) is given by [18, 19]

$$\frac{B_2}{V} = 1 + 3\alpha, \tag{1}$$

$$\alpha = \frac{(RS)}{3V}, \tag{2}$$

where B_2 is the second virial coefficient, α the non-sphericity of the molecule and R, S, and V the mean radius of curvature, surface and volume of the hard ellipsoid respectively. The exact expressions for R, S and V of a hard ellipsoid are given in [19].

Although the second virial coefficient can be computed easily from equations (1)–(2), the evaluation of higher virial coefficients must be performed numerically. We have evaluated the third, fourth and fifth virial coefficient of ellipsoids of different geometries by using the method of Ree and Hoover [24] as extended to molecular fluids by Rigby [25]. Typically, we used five million configurations for the less anisotropic molecules and ten million for the most anisotropic ones. Each configuration is totally independent from the previous one, so that we are using a static scheme for generating the open chain configurations (see [26] for details). The estimated error was given as twice the standard deviation of 10 subaverages. We used the procedure proposed by Perram and Wertheim [27] for detecting overlapping between the ellipsoidal molecules.

For computing the EOS of hard ellipsoids we used *NPT* Monte Carlo simulations [28, 29] with 108 and in a few cases with 256 particles. The shape of the box was cubic and we used isotropic scaling so that it remained cubic during the simulation. We expect this to be adequate for studying the isotropic phase. We typically used 2×10^6 configurations for equilibration and 2×10^6 configurations to obtain averages. We started at a very low pressure from a solid which melts very quickly, and then compressed the sample by increasing the pressure. Orientational order parameters were also determined to be sure that all our simulations were in the isotropic phase. Displacements in the position of particles and volume of the system were chosen so that 40% of the trial moves were accepted. Theoretical estimates of the location of the isotropic–nematic transition of hard spheroids were very helpful as an approximate guide of the range of densities were the isotropic phase is thermodynamically stable.

3. Results for the virial coefficients

In table 1, virial coefficients for ellipsoids with $c = 3$ are presented. Results range from $b = 1$ (prolate spheroid) to $b = 3$ (oblate spheroid). For the prolate and oblate spheroids the virial coefficients of this work were compared with those previously reported by Rigby [6]. Good agreement was found which constituted a cross check of the calculations. The numerical procedure used to determine the virial coefficients yields a numerical estimate of the second virial coefficient of the model.

Table 1. Virial coefficients for $c = 3$ and several values of b. These virial coefficients were calculated using 5 million independent configurations. Reduced virial coefficients B_i^* are defined as $B_i^* = B_i / V^{i-1}$, where V is the molecular volume. The values in parentheses in the column labelled as B_2^* are the exact values of the second virial coefficients as calculated from the exact expression given by equations (1), (2). For the prolate and oblate spheroids the estimated error of the calculations has been included.

b	B_2^*	B_3^*	B_4^*	B_5^*
1	5·4516 (5·4537)	$15{\cdot}82 \pm 0{\cdot}01$	$27{\cdot}0 \pm 0{\cdot}1$	36 ± 2
1·0909	5·3361 (5·3364)	15·34	26·5	36
1·20	5·2324 (5·2329)	14·94	26·1	35
1·25	5·1951 (5·1963)	14·80	26·0	36
1·3333	5·1478 (5·1476)	14·63	25·9	36
1·5	5·0866 (5·0868)	14·45	25·82	35
1·7143	5·0596 (5·0608)	14·44	26·2	35
$(3)^{1/2}$	5·0605 (5·0607)	14·48	26·3	35
1·75	5·0606 (5·0608)	14·46	26·3	35
2	5·0864 (5·0868)	14·70	27·0	36
2·25	5·1480 (5·1476)	15·08	28·0	37
2·5	5·2330 (5·2329)	15·55	29·0	38
2·75	5·3358 (5·3364)	16·11	30·2	38
3	5·4546 (5·4537)	$16{\cdot}74 \pm 0{\cdot}01$	$31{\cdot}5 \pm 0{\cdot}1$	39 ± 1

In table 1 we show both, the numerical estimate and the exact value obtained from equations (1)–(2). Again, good agreement is found thus giving further confidence in our calculations.

We see that the second virial coefficients of biaxial ellipsoids are lower than these of the prolate or oblate spheroids. According to equations (1)–(2) this means that biaxial ellipsoids are more spherical than uniaxial ones (for a given fixed value of c). It can be seen in table 1 that the second virial coefficient of a model with $1 : b : c$ is identical to that of the model with $1 : c/b : c$. A consequence of that is the prolate–oblate symmetry presented by the second virial coefficient of hard ellipsoids. The model with $1 : c^{1/2} : c$ is invariant under this transformation and for this value of b the second virial coefficient of the ellipsoid is a minimum. Therefore, one concludes (see equations (1)–(2)) that the non-sphericity parameter of hard ellipsoids $1 : b : c$ with c fixed and b ranging from 1 to c reaches a minimum when $b = c^{1/2}$. This has been known for some time [14, 16]. For a given value of c, we can say that hard ellipsoids $1 : b : c$ with $b < c^{1/2}$ are prolate-like, whereas ellipsoids with $b > c^{1/2}$ are oblate-like. In what follows we shall denote a hard ellipsoid as prolate when $b < c^{1/2}$ and as oblate when $b > c^{1/2}$. The ellipsoid with $1 : 1 : c$ will be denoted as the prolate spheroid whereas this with $1 : c : c$ it will be denoted as the oblate spheroid.

The third virial coefficient follows to some extent the trends of the second virial coefficient. In fact, biaxial molecules present in general lower values of the third virial coefficient than either the prolate or the oblate spheroids. However, there are two important differences between the behaviour of the second and the third virial coefficient. It is seen that the prolate–oblate symmetry is now broken and oblate ellipsoids present higher values of the third virial coefficient than prolate ones. Moreover, the minimum in the third virial coefficient is no longer located at $1 : c^{1/2} : c$ but is shifted towards prolate molecules. For the fourth and fifth virial coefficient it is seen that biaxiality has only a small effect on the value of the virial coefficient. There is a weak minimum in the value of the fourth and fifth virial coefficient located in the prolate region and the value of these two coefficients for oblate molecules is higher than for prolate ones.

Table 2. Virial coefficients for $c = 4$ and several values of b. The virial coefficients were calculated by using 5 million configurations. Rest of the notation as in table 1.

b	B_2^*	B_3^*	B_4^*	B_5^*
1	6·4763 (6·4779)	20·28	30·5	37
1·1429	6·2269 (6·2280)	19·20	30·1	37
1·3333	6·0139 (6·0133)	18·37	29·9	36
2	5·7846 (5·7842)	17·92	31·7	36
3	6·0121 (6·0132)	19·72	36·9	38
3·5	6·2283 (6·2280)	21·08	39·9	35
4	6·4780 (6·4779)	22·64	43·2	35

In table 2 results for the virial coefficients of hard ellipsoids with $c = 4$ are presented. Trends in the second and third virial coefficient are similar to those previously discussed for $c = 3$. The fourth virial coefficient of the prolate spheroid is smaller than this of the oblate one. As can be seen in table 2 a weak minimum is found for the fourth virial coefficient when $c = 4$. The fifth virial coefficient seems to depend very little on b for $c = 4$. Although the uncertainty of the results does not allow a definitive conclusion, it seems that the fifth virial coefficient decreases when going from the prolate spheroid to the oblate one.

In tables 3 and 4 the virial coefficients for $c = 5$ and 7 are presented. For the second and third, trends are similar to these previously discussed for $c = 3$. The third virial coefficient of the oblate spheroid is higher than that of the prolate one. It is clear that the differences between prolate and oblate molecules in the third virial coefficient increase as the value of c increases. The fourth virial coefficient increases monotonously when going from prolate molecules to oblate ones. The variation now seems to be quite pronounced. The fifth virial coefficient decreases monotonously when going from prolate molecules to oblate ones.

Table 3. Virial coefficients for $c = 5$ and several values of b calculated with 10 million configurations. For the prolate and oblate spheroids the estimated error of the calculations has been included. Rest of the notation as in table 1.

b	B_2^*	B_3^*	B_4^*	B_5^*
1	7·5540 (7·5520)	25·28 ± 0·02	31·2 ± 0·2	41 ± 3
1·25	7·0438 (7·0453)	23·02	31·8	38
1·6666	6·6588 (6·6580)	21·70	33·7	32
2	6·5491 (6·5485)	21·59	35·5	33
$(5)^{1/2}$	6·5286 (6·5303)	21·78	36·90	30
2·5	6·5495 (6·5485)	22·18	38·7	30
3	6·6586 (6·6580)	23·25	42·2	32
4	7·0463 (7·0453)	26·22	49·8	25
5	7·5529 (7·5520)	29·88 ± 0·02	57·8 ± 0·2	9 ± 5

Table 4. Virial coefficients for $c = 7$ and several values of b calculated with 10 million configurations. Rest of the notation as in table 1.

b	B_2^*	B_3^*	B_4^*	B_5^*
1	9·7748 (9·7737)	36·21	19·1	107
1.1666	9·2338 (9·2307)	33·59	24·3	70
1·5	8·5936 (8·5921)	30·98	31·2	41
$(7)^{1/2}$	8·0480 (8·0471)	30·65	46·3	8
4·6666	8·5935 (8·5921)	37·17	69·4	- 41
6	9·2306 (9·2307)	43·06	84·6	- 87
7	9·7734 (9·7737)	48·02	95·8	- 150

In table 5 the virial coefficients for $c = 10$ are presented. The studied values of b are those considered by Allen in his Monte Carlo (MC) study. Trends in the second and third virial coefficient are similar to those previously discussed. When going from prolate molecules to oblate ones the fourth virial coefficient increases monotonously while the fifth virial coefficient decreases. As can be seen in table 5, the fourth virial coefficient of the prolate spheroid with $c = 10$ is negative, whereas for this elongation the fifth virial coefficient of the oblate spheroid is negative. It is well known that prolate molecules with high anisotropy present negative values of the fourth virial coefficient [6, 30], whereas oblate molecules of high anisotropy present negative values of the fifth virial coefficient [31]. For $c = 7$ (see table 4), the fifth virial coefficient is negative for the oblate spheroid whereas the fourth virial coefficient of the prolate spheroid is still positive. It is thus seen that prolate molecules only reach negative values of the fourth virial coefficient for large anisotropies, whereas oblate molecules already present negative values of the fifth virial coefficient for moderate anisotropies. For the invariant point $1 : 10^{1/2} : 10$ the fifth virial coefficient is negative, whereas the fourth one is positive (see table 5).

In figures 1–4 a plot of B_2, B_3, B_4 and B_5 for $c = 3$ and $c = 10$ are presented. The value of b is plotted on a logarithmic scale so that for each ellipsoid the middle point of the curve corresponds to the invariant ellipsoid. The general image emerging from figures 1–4 is that prolate and oblate ellipsoids do not differ much in their virial coefficients for moderate anisotropies ($c = 3$) but they are quite different when the anisotropy of the molecule is large ($c = 10$). The shape of the plots for B_2 and B_3 versus $\ln(b)$ is roughly parabolic, presenting a minimum for a medium value of b. For B_4 and B_5 the variation of the virial coefficient with $\ln(b)$ is approximately linear.

The results presented so far may be useful for checking the quality of different methods developed to estimate the virial coefficients of hard convex bodies

Table 5. Virial coefficients for $c = 10$ and several values of b calculated with ten million configurations. The values in parentheses in the columns of B_3^*, B_4^* and B_5^* are virial coefficients of hard spheroids as reported by Rigby [6]. For the prolate and oblate spheroids the estimated error of the calculations has been included. Rest of the notation as in table 1.

b	B_2^*	B_3^*	B_4^*	B_5^*
1	13·193 (13·1913)	54·59 ± 0·04 (54·66)	- 43·4 ± 0·6 (- 43·3)	652 ± 35 (614)
1·259	12·062 (12·0606)	48·76	- 14·3	347
1·585	11·264 (11·2628)	45·54	5·9	174
2	10·731 (10·7316)	44·24	21·7	59
2·5	10·442 (10·4403)	44·60	36·5	- 23
2·818	10·362 (10·3634)	45·29	44·4	- 62
$(10)^{1/2}$	10·340 (10·3392)	46·35	52·0	- 108
3·548	10·364 (10·3633)	47·75	60·7	- 135
4	10·439 (10·4403)	49·57	70·2	- 179
5	10·733 (10·7316)	54·29	89·7	- 255
6.31	11·263 (11·2632)	61·17	114·5	- 399
7·943	12·059 (12·0607)	70·90	143·8	- 587
10	13·189 (13·1913)	84·53 ± 0·05 (84·51)	179·1 ± 0·9 (177·2)	- 950 ± 31 (- 1004)

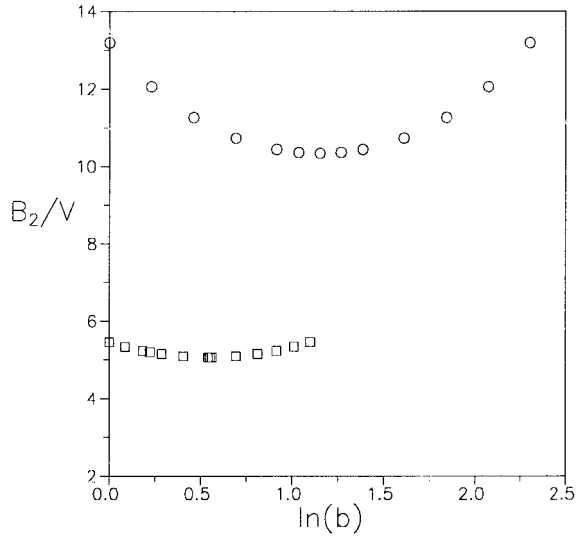

Figure 1. Reduced second virial coefficient of hard ellipsoids plotted as a function of $\ln(b)$. Squares: ellipsoids with $c = 3$, circles: ellipsoids with $c = 10$.

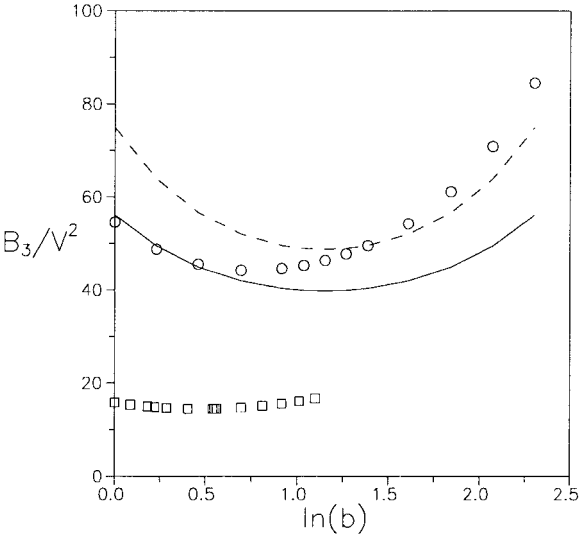

Figure 2. Reduced third virial coefficient of hard ellipsoids as a function of $\ln(b)$. Symbols correspond to the virial coefficients computed in this work. Squares: ellipsoids with $c = 3$, circles: ellipsoids with $c = 10$. Lines correspond to virial coefficients of hard ellipsoids with $c = 10$ as estimated from the EOS of Nezbeda (solid line) and Song and Mason (dashed line).

[32] However, an important limitation is that in this work we have considered only a small set of all the possible geometries of hard ellipsoids. It would be useful to have an empirical expression which fits the virial coefficients of the hard ellipsoids provided in this work so that a guess of the virial coefficients of hard ellipsoids not considered in this work can be obtained. Such an empirical expression is given in the next section.

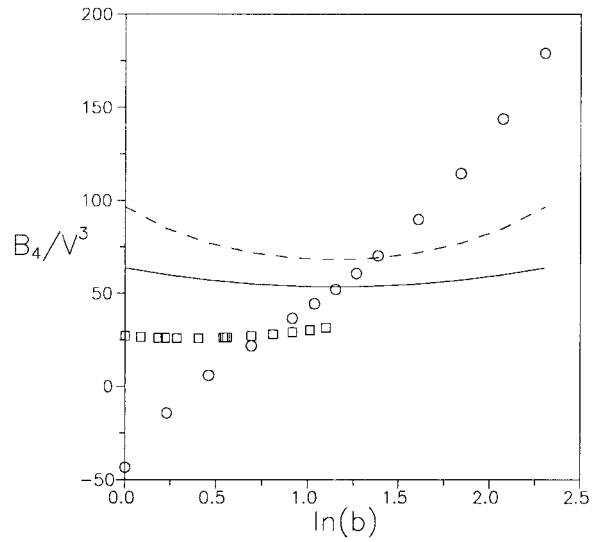

Figure 3. Reduced fourth virial coefficient of hard ellipsoids as a function of $\ln(b)$. Symbols correspond to the virial coefficients computed in this work. Squares: ellipsoids with $c = 3$, circles: ellipsoids with $c = 10$. Lines correspond to virial coefficients of hard ellipsoids with $c = 10$ as estimated from the EOS of Nezbeda (solid line) and Song and Mason (dashed line).

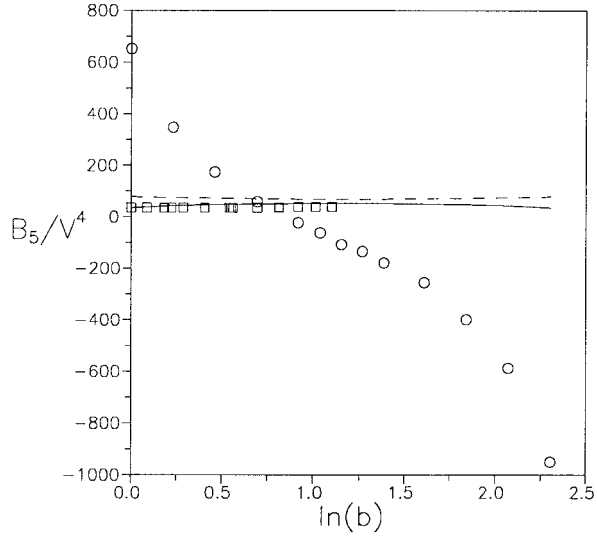

Figure 4. Reduced fifth virial coefficient of hard ellipsoids as a function of $\ln(b)$. Symbols correspond to the virial coefficients computed in this work. Squares: ellipsoids with $c = 3$, circles: ellipsoids with $c = 10$. Lines correspond to virial coefficients of hard ellipsoids with $c = 10$ as estimated from the EOS of Nezbeda (solid line) and Song and Mason (dashed line).

4. Empirical expression for the virial coefficients of hard ellipsoids: application to other convex bodies

The goal of this section is rather simple. We seek an empirical expression which fits the virial coefficients of

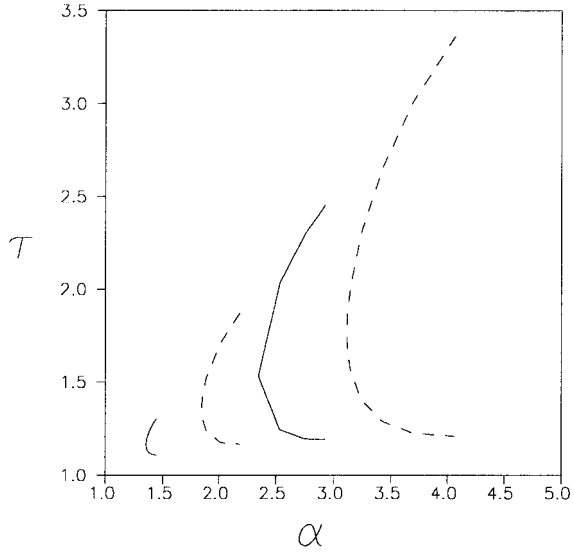

Figure 5. Values of α and τ for hard ellipsoids. From left to right, the lines correspond to hard ellipsoids with $c = 3$ (solid line), $c = 5$ (dashed line), $c = 7$ (solid line) and $c = 10$ (dashed line). Prolate spheroids are located in the top, whereas oblate spheroids are in the bottom.

hard ellipsoids presented in the previous section. For that purpose we shall use some concepts of convex body geometry (see [26, 33] for further details on convex body geometry). A convex body is defined as that in which any line connecting two points within the body is also fully contained within the body. For hard convex bodies we have the following Minkowski's inequalities [34] which can be written as

$$4\pi R^2 - S \geqslant 0, \tag{3}$$

$$(4\pi R)^3 - 3(4\pi)^2 V \geqslant 0, \tag{4}$$

$$S^2 - 12\pi RV \geqslant 0. \tag{5}$$

From these inequalities one can define the following parameters:

$$\tau = \frac{4\pi R^2}{S} \geqslant 1, \tag{6}$$

$$\lambda = \frac{4\pi R^3}{3V} \geqslant 1. \tag{7}$$

Using these definitions and that of α from equation (2) it is easy to show that [35]:

$$\alpha \geqslant \tau, \tag{8}$$

$$\alpha = \frac{\lambda}{\tau}. \tag{9}$$

From equation (9) it is clear that once α and τ are known then λ can be easily obtained. For a sphere, α and τ are unity. For any other convex body α and τ are larger than unity. The parameter τ was also used previously by Naumann and Leland [36] in their search for a general equation of state for hard convex bodies. The value of α for a prolate spheroid with $1 : 1 : c$ is identical to that of an oblate spheroid with $1 : c : c$. However, the prolate spheroid presents a larger value of τ than the oblate one. Thus, the parameter τ distinguishes between prolate and oblate molecules. In figure 5 the values of α and τ for the hard ellipsoids considered in this work are plotted. For a given value of c, the value of τ increases continuously from the oblate spheroid to the prolate one. It has been recognized for some time, that the parameter α is not sufficient to describe the virial coefficients of hard convex bodies. The need for a second (or maybe third ...) parameter to describe the virial coefficient data of hard convex bodies has been advocated. In any case it should be recognized that molecular shape (which is given by a function defining the surface of the body) cannot be summarized in a few non-sphericity parameters without losing information. It is not likely that any virial coefficient of hard convex bodies can be given exactly by a few non-sphericity parameters. However, we want to explore here the possibility of correlating the virial coefficient of hard ellipsoids by using only two non-sphericity parameters, namely α and τ. We have fitted successfully all the virial coefficient data presented in the previous section to the following expressions:

$$\frac{B_3}{V^2} = 10 + 13{\cdot}094\,756\alpha' - 2{\cdot}073\,909\tau' + 4{\cdot}096\,689\alpha'^2 - 5{\cdot}791\,266\alpha'\tau' + 2{\cdot}325\,342\tau'^2, \tag{10}$$

$$\frac{B_4}{V^3} = 18{\cdot}3648 + 27{\cdot}714\,434\alpha' - 10{\cdot}204\,600\tau' + 11{\cdot}142\,963\alpha'^2 + 8{\cdot}634\,491\tau'^2 - 28{\cdot}279\,451\alpha'\tau' - 17{\cdot}190\,946\alpha'^2\tau' + 24{\cdot}188\,979\alpha'\tau'^2 + 0{\cdot}746\,746\alpha'^3 - 9{\cdot}455\,150\tau'^3, \tag{11}$$

$$\frac{B_5}{V^4} = 28{\cdot}2245 + 21{\cdot}288\,105\alpha' + 4{\cdot}525\,788\tau' + 36{\cdot}032\,793\alpha'^2 + 59{\cdot}009\,800\tau'^2 - 118{\cdot}407\,497\alpha'\tau' + 24{\cdot}164\,622\alpha'^2\tau' + 139{\cdot}766\,174\alpha'\tau'^2 - 50{\cdot}490\,244\alpha'^3 - 120{\cdot}995\,139\tau'^3 + 12{\cdot}624\,655\alpha'^3\tau', \tag{12}$$

where we have defined α' and τ' as:

$$\alpha' = \alpha - 1 \tag{13}$$

Table 6. Virial coefficients for hard ellipsoids $1 : b : c$ as obtained from equations (10)–(12) (Fit) and from the calculations of this work (Exact).

b	c	B_3^* (Exact)	B_3^* (Fit)	B_4^* (Exact)	B_4^* (Fit)	B_5^* (Exact)	B_5^* (Fit)
1	3	15·82	15·93	27·0	27·1	36	36
$(3)^{1/2}$	3	14·48	14·53	26·3	26·3	35	35
3	3	16·74	16·79	31·5	31·6	39	38
1	5	25·28	25·23	31·2	31.0	41	40
$(5)^{1/2}$	5	21·78	21·77	36·9	36·8	30	33
5	5	29·88	29·82	57·8	57·7	9	12
1	10	54·59	54·74	- 43·4	- 43·5	652	651
$(10)^{1/2}$	10	46·35	46·38	52·0	52·3	- 108	- 104
10	10	84·53	84·54	179·1	179·0	- 950	- 952

Table 7. Virial coefficients for hard spherocylinders as obtained from equations (10)–(12) (Fit) compared with the exact values as reported in [30, 37–39] The length to breadth ratio of the hard spherocylinder is given by $L^* + 1$.

L^*	B_3^* (Exact)	B_3^* (Fit)	B_4^* (Exact)	B_4^* (Fit)	B_5^* (Exact)	B_5^* (Fit)
Prolate						
1	12·34	12·41	22·5	22·5	32	32
3	20·43	20·36	31·9	31·0	40	36
5	29·68	29·61	31·4	30·2	55	47
10	56·05	57·09	- 37·6	- 44·9	733	627
100	745	1562	- 32 112	- 97 088	$3·7 \times 10^6$	11×10^6
Oblate						
1	11·65	11·65	21·8	21·6	33	31
3	18·67	18·60	36·5	35·6	44	39
5	28·24	28·09	57·5	55·1	38	21
10	61·65	61·77	128·2	129·1	- 343	- 383

$$\tau' = \tau - 1. \tag{14}$$

In table 6 the virial coefficients of hard ellipsoids as obtained from equations (10)–(12) are compared with the numerical results of this work, presented in the previous section. As can be seen, the fitting provided by equations (10)–(12) is extremely good. The usefulness of equations (10)–(12) is that they allow for an estimate of the virial coefficients of hard ellipsoids, even for values of $a : b : c$ for which no numerical estimate is available.

One question which may arise after looking at equations (10)–(12) is whether they could be used to estimate virial coefficients of any kind of convex body. Equations (10)–(12) were obtained by fitting the virial coefficients of hard ellipsoids only, but it would be interesting to see whether they can predict correctly the virial coefficients of other kinds of convex bodies. After all, the second virial coefficient depends on α only, so that the idea that two parameters, say α and τ, may provide estimates of higher virial coefficients, seems appealing. In table 7 we present results from the virial coefficients of hard spherocylinders obtained numerically [30, 37–39] and from equations (10)–(12). Equations (10)–(12) were obtained by fitting virial coefficient data of hard ellipsoids with a maximum length to breadth ratio of 10. It is seen in table 7 that for hard spherocylinders (prolate and oblate) with a similar anisotropy (i.e. length to breadth ratio) equations (10)–(12) provide excellent results. To check the possibilities of extrapolating equations (10)–(12) to much higher anisotropies we have included in table 7 results for a prolate spherocylinder with a length to breadth ratio of about 100. As can be seen the results now deteriorate, indicating that equations (10)–(12) should be used with caution for very large anisotropies (i.e. length to breadth ratios). In any case the results of table 7 show that equations (10)–(12) can be used with confidence to get reliable estimates of the virial coefficients of hard ellipsoids and hard spherocylinders with a length to breadth ratio equal to or smaller than 10.

Taking equations (10)–(12) one step further, we can use them to predict the virial coefficients for hard convex bodies for which no previous estimate is so far available,

Table 8. Virial coefficients for hard spheroplatelets $1 : b : c$ as obtained from equations (10)–(12) (fit). The definition of $a : b : c$ as in figure 1 of [15]. The parameters b and c define the size of the rectangle. The spheroplatelet is obtained by sliding a sphere of diameter a over the rectangle. We take a as the unit length so that $a = 1$. For the cylinder we take the diameter of the circle as the unit of length, i.e. $b = 1$, and the height of the cylinder is c.

b	c	B_3^*	B_4^*	B_5^*
Spheroplatelets				
1	1	11·08	20·4	30
2	2	12·92	23·7	33
1	3	13·49	24·4	34
4	4	17·46	31·8	37
1	25	59·38	- 42·1	538
10	10	36·28	62·9	- 35
Cylinders				
1	1	13·72	25·3	34
1	3	19·98	31·6	36
1	10	55·99	- 37·7	547
1	0·1	60·64	127·8	- 359

for instance, hard cylinders and spheroplatelets. Predictions for these two kinds of convex bodies are presented in table 8. As can be seen, equation (11) predicts the existence of negative fourth virial coefficients for prolate-like cylinders and for prolate-like spheroplatelets. Equation (12) predicts the existence of negative fifth virial coefficients for oblate-like spheroplatelets and oblate-like cylinders. It seems that negative values of the fourth virial coefficient are the signature of prolate-like molecules, whereas negative fifth virial coefficients are the signature of oblate-like molecules. The second virial coefficient of hard cylinders and hard spheroplatelets are well known [15, 37]. However, to our knowledge, no data has been so far presented for higher virial coefficients of hard spheroplatelets or hard cylinders so that the results presented in table 8 constitute a first estimate. It is difficult to assess the accuracy of equations (10)–(12) for hard cylinders and hard spheroplatelets, but taking into account the accuracy of equations (10)–(12) for ellipsoids and spherocylinders, in principle, one should expect that the predictions are not too bad.

Can it be claimed that a general (although empirical) expressions has veen found for the virial coefficients up to the fifth of hard convex bodies? Our feeling is that the answer to this question is no. In table 9 the virial coefficients for a hard cube as obtained from equations (10)–(12) are compared with the value obtained numerically by Nezbeda and Boublík [40]. As can be seen, the agreement now is rather poor. Therefore equations (10)–(12) do not provide a successful expression for the virial

Table 9. Virial coefficients for a hard cube as obtained from equations (10)–(12) (Fit) and from the numerical calculations of [40].

B_3^* Exact	B_3^* Fit	B_4^* Exact	B_4^* Fit	B_5^* Exact	B_5^* Fit
18·33	16·76	42	31	*	37

coefficients of any type of convex body. We already anticipated that it is hard to believe that shape, which is described by a function defining the surface of the convex body, can be condensed into a few parameters without losing some essential information. It seems that within a certain family of convex bodies (i.e. ellipsoids and spherocylinders) it is possible to obtain reliable estimates of the virial coefficients up to the fifth using a unique expression depending on α and τ. However, this expression can fail completely when applied to other families of convex bodies as is the case with a hard cube. After these words of caution one should admit that the existence of a general (although empirical) expression for the virial coefficients of hard ellipsoids (including prolate spheroids, oblate spheroids, and biaxial ellipsoids) and hard spherocylinders (including prolate and oblate ones) is good news. The shape of many molecules can be approximately described by these geometries, so that equations (10)–(12) may be useful in the search for an equation of state of hard convex bodies. We explored also the possibility of using equations (10)–(12) for hard non-convex bodies, such as linear chains of tangent hard spheres (by taking the mean radius of curvature, which is ill-defined for non-convex bodies, from that of a spherocylinder of the same length to breadth ratio) but the results were poor. Therefore equations (10)–(12) should only be used for convex bodies, and within the family of convex bodies for ellipsoids and spherocylinders. It is likely that equations (10)–(12) should provide good estimates for cylinders and spheroplatelets, but we do not have results for these models to check this point.

5. Equation of state for hard ellipsoids

The results presented so far illustrate that in general, for a given value of c, the virial coefficients of prolate ellipsoids differ substantially from those of oblate ellipsoids. One should expect that this difference will be reflected in the equation of state. To analyse this in further detail we have performed MC simulations for several values of c and b. The EOS for prolate and oblate hard spheroids with $c \leqslant 3$ has been obtained by computer simulations by Frenkel and Mulder [5]. For $c = 10$ Allen [16] has obtained the EOS for several

Table 10. MC results for the EOS of hard ellipsoids with $c = 3$ and several values of b. The reduced number density ρ^* is defined as $\rho^* = (N/V')d_{HS}^3$ where N is the number of particles, V' is the volume of the system and d_{HS} is the diameter of a hard sphere with the same volume as the hard ellipsoid. The volume of the ellipsoid is given by $V = (\pi/6)abc$. The reduced pressure p^* is defined as $p^* = p/(kT/d_{HS}^3)$. The compressibility factor is given by $Z = p/(\rho kT)$, where ρ is the number density of the hard spheroid.

	$b = 1$		$b = 1{\cdot}7320$		$b = 3$	
p^*	ρ^*	Z	ρ^*	Z	ρ^*	Z
1	0·352	2·84	0·365	2·74	0·350	2·86
2	0·481	4·16	0·499	4·01	0·485	4·12
3	0·568	5·28	0·583	5·15	0·575	5·22
4	0·635	6·30	0·652	6·13	0·626	6·39
5	0·676	7·40	0·697	7·17	0·674	7·42
6	0·721	8·32	0·730	8·22	0·712	8·43
8	0·785	10·19	0·790	10·13	0·784	10·20
10	0·830	12·05	0·845	11·83	0·825	12·12
12	0·869	13·81	0·891	13·47	0·864	13·89

Table 11. MC results for the EOS of hard ellipsoids with $c = 4$ and several values of b. Rest of the notation as in table 10.

	$b = 1$		$b = 2$		$b = 4$	
p^*	ρ^*	Z	ρ^*	Z	ρ^*	Z
1	0·331	3·02	0·354	2·82	0·331	3·02
2	0·465	4·30	0·464	4·31	0·459	4·36
3	0·540	5·56	0·553	5·42	0·528	5·68
4	0·599	6·68	0·614	6·51	0·584	6·85
5	0·650	7·69	0·669	7·47	0·640	7·81
6	0·685	8·76	0·698	8·60	0·682	8·80
7	0·716	9·78	0·754	9·28	0·729	9·60
8	0·754	10·61	0·767	10·43	0·753	10·62

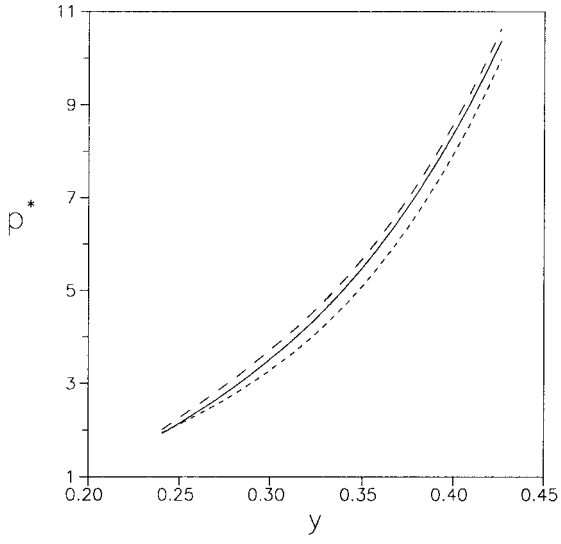

Figure 6. Simulation results for the equation of state of hard ellipsoids with $c = 4$ as a function of the volume fraction, y. For the definition of y, see equation (18) of the main text. Solid line: prolate spheroid, dashed line: oblate spheroid, short-dashed line: invariant ellipsoid.

Table 12. MC results for the EOS of hard ellipsoids with $c = 5$ and several values of b. Results for $b = 1$ and $b = 5$ were obtained from simulations with 256 particles. Rest of the notation as in table 10.

	$b = 1$		$b = 2{\cdot}2361$		$b = 5$	
p^*	ρ^*	Z	ρ^*	Z	ρ^*	Z
1	0·320	3·12	0·337	2·96	0·307	3·26
2	0·437	4·58	0·450	4·45	0·426	4·69
3	0·515	5·83	0·533	5·63	0·501	5·99
4	0·573	6·98	0·588	6·80	0·559	7·16

values of b. Therefore, in this work we focus on hard ellipsoids with c in the range 3, 10. In particular, we shall consider the values $c = 3$, 4 and 5. In tables 10, 11 and 12 the MC results for $c = 3$, 4 and 5 are presented. For each value of c, we shall consider three values of b corresponding to the prolate spheroid, the oblate spheroid and the invariant ellipsoid. For the prolate spheroid with $c = 3$ we compared our simulation results with those previously obtained by Frenkel and Mulder [5] and the agreement was found to be excellent.

From the results of tables 10–12 it can be seen that for a given pressure, the densities of the prolate spheroid, oblate spheroid and invariant ellipsoids are quite similar. This is quite surprising, especially when one considers the important differences in the virial coefficients shown in tables 1–5. However, some differences in density between the ellipsoids with the same value of c are clearly visible. For instance, let us consider the results for $c = 4$. It is found that for a given pressure, the density increases when going from the prolate spheroid to the invariant ellipsoid, reaching a maximum and then decreasing again for the oblate spheroid. It is also found that for a given pressure, the density of the oblate spheroid is lower than that of the prolate one. This is further illustrated in figure 6 where the reduced pressure p^* is plotted as a function of the volume fraction, y, for different hard ellipsoids with $c = 4$. The volume fraction y is defined as the number density times the molecular volume (see equation (18) later). It is probably more useful to discuss trends in the compressibility factor for a given volume fraction, however. For

a given volume fraction, the lowest value in the compressiblity factor corresponds to the invariant ellipsoid, and the largest to the oblate spheroid, while the value of the prolate spheroid is intermediate between the other two. Results for other elongation are quite similar to those presented for $c = 4$. It is difficult to relate the behaviour found for the compressibility factor with that of the virial coefficients. However, a qualitative discussion is possible. The trend found in the compressibility factor can be obtained correctly by considering only the second and third virial coefficients. In fact, the invariant ellipsoid always has a smaller value of the second and third virial coefficients than the prolate and oblate spheroids. Therefore, it is not surprising that it has the lowest value in the compressibility factor for a given density. Prolate and oblate spheroids have the same value of the second virial coefficient [14, 37]. However, oblate spheroids have higher values of the third virial coefficient than prolate ones. Therefore, it is not surprising that the compressibility factor of oblate spheroids is always larger than that of prolate spheroids. To summarize, the trends in the compressibility factor for a given volume factor can be qualitatively understood by considering only the second and third virial coefficients. What it is not so simple to understand is why the differences in the compressibility factor between prolate spheroids, oblate spheroids and invariant spheroids are relatively small. Frenkel and Mulder [5] already found that the EOSs for prolate and oblate spheroids are quite similar when $c < 3$. Even admitting that this is a surprising result, an explanation of this can be obtained when one compares the virial coefficients of prolate and oblate spheroids for $c = 3$ presented in table 1. Prolate and oblate spheroids of moderate anisotropy do not differ much in their virial coefficients. It is not therefore surprising that they present a similar EOS. However, Allen [16] has recently shown that even for highly anisotropic molecules ($c = 10$) the EOS for prolate and oblate spheroids are quite similar. The results presented in this work for $c = 4$, 5 and 7 provide further evidence of this. It is hard to understand the origin of this point. Differences in the third, fourth and fifth virial coefficients for these anisotropies are quite pronounced. Why are they not reflected in the EOSs? We have found that the explanation of this relies on the values of the fourth and fifth virial coefficients. Let us consider the virial coefficients for $c = 10$ presented in table 5. Whereas the contribution to the pressure of the fourth virial coefficient is negative for prolate spheroids (see table 5) and positive for oblate spheroids, the contribution of the fifth virial coefficient is positive for prolate spheroids and negative for oblate spheroids. For $c = 10$ the contribution to the pressure arising from the fourth and fifth virial coefficients becomes identical for prolate and oblate spheroids when the volume fraction is approximately $y = 0{\cdot}14$. This is not too far from the isotropic–nematic transition, which is expected to occur when $y = 0{\cdot}20$ approximately [41]. For densities higher than $y = 0{\cdot}14$, the contribution of the fourth and fifth coefficients is higher for the prolate spheroid than for the oblate one and this compensates partially for the difference in the third virial coefficient. For the invariant ellipsoid the contribution of the fourth and fifth virial coefficient together at densities higher than $y = 0{\cdot}14$ is intermediate between that of prolate and oblate spheroids. Therefore, the large differences between the oblate spheroid and the invariant ellipsoid generated by the second and third virial coefficients are reduced at high densities, when the contribution of the fourth and fifth virial coefficient is included.

It should be remembered that the density at which the nematic phase occurs decreases as the anisotropy of the molecule increases [3]. If the isotropic–nematic transition did not occur, differences in the EOS of prolate and oblate spheroids with large values of c would be quite important at high densities. Therefore, to explain the similarity in the EOS for prolate and oblate spheroids for large values of c the following facts are relevant. (i) The density at which the isotropic–nematic transition occurs decreases as the anisotropy of the molecule increases. (ii) The second virial coefficient is identical for both models. (iii) The third virial coefficient of the oblate spheroid is higher than that of the prolate one. (iv) The contribution of the fourth and fifth virial coefficients are of different sign for prolate and oblate spheroids but the sum of both turns out to be the same for a density smaller but not too far from the density at which the isotropic–nematic transition occurs. (v) For higher densities, the contribution of the fourth and fifth virial coefficients together is higher for prolate than for oblate spheroids and this compensates partially the differences in the third virial coefficient.

Therefore, the prolate–oblate symmetry found in the EOS for hard spheroids with moderate anisotropy (i.e. $c < 3$) is due to the similarity in the virial coefficients of both types of molecules. When the ellipsoids are very anisotropic, the prolate–oblate symmetry is due to the fact that the joint contribution of the fourth and fifth virial coefficients is quite similar for prolate and oblate spheroids for those densities close to the isotropic–nematic transition. The invariant ellipsoid would present in general smaller values of the compressibility factor for a given density than prolate or oblate spheroids, due to the smaller value of the second and third virial coefficients. However, since the contribution of the fourth and fifth virial coefficients for the invariant ellipsoid is intermediate between those of the prolate and

oblate spheroids, the differences in the EOS with these other two models will never be too large.

In our discussion we have not taken into account the contribution of virial coefficients larger than the fifth. However, for large values of c the contribution of higher virial coefficients to the EOS at the densities at which the isotropic phase is stable is not very large.

Once the virial coefficient and the EOS for ellipsoids have been presented, let us discuss which among several EOSs proposed for hard convex bodies provides a better description of the simulation data. We shall consider the EOS proposed by Nezbeda [20], hereinafter denoted as Nezbeda EOS which is given by

$$Z = \frac{p}{\rho k T} = \frac{1 + (3\alpha - 2)y + (\alpha^2 + \alpha - 1)y^2 - \alpha(5\alpha - 4)y^3}{(1 - y)^3}, \tag{15}$$

where α is the non-sphericity parameter defined in equation (2). An EOS recently proposed for hard convex bodies is that of Song and Mason [23]

$$Z = \frac{1 + (3\alpha - 2)y + (3\alpha^2 - 3\alpha + 1)y^2 + \alpha(6{\cdot}3648 - 7\alpha)y^3}{(1 - y)^3}. \tag{16}$$

Another EOS very commonly used in theoretical studies of the isotropic–nematic transition of convex bodies is that proposed by Parsons [22] which is given by

$$Z = 1 + \frac{B_2}{4}(Z_{\mathrm{HS}} - 1) = 1 + \frac{B_2}{4}\left(\frac{1 + y + y^2 - y^3}{(1 - y)^3} - 1\right), \tag{17}$$

where Z_{HS} is the compressibility factor of hard spheres which in this work will be described by the Carnahan–Starling [42] EOS. In equations (15)–(17) y stands for the volume fraction defined as

$$y = \rho V = \frac{N}{V'} V \tag{18}$$

where ρ is the number density, N the number of particles, V' the volume of the system and V the molecular volume.

In tables 13–16 the simulation results are compared with those of these three analytical EOSs for c = 3, 4, 5, 10 and several values of b. In the last row the average deviation between simulation and theoretical predictions, Δ, defined as

$$\Delta = 100\frac{1}{n_{\mathrm{MC}}}\sum_{i=1}^{i=n_{\mathrm{MC}}}\frac{|Z^i_{\mathrm{MC}} - Z^i_{\mathrm{theo}}|}{Z^i_{\mathrm{MC}}}, \tag{19}$$

are presented. In equation (19) n_{MC} stands for the number of simulation points, and Z^i_{MC} and Z^i_{theo} stand for the simulation and theoretical value of the compressibility factor for state point i respectively. The average deviation obtained for all the values of c and b presented in tables 13–16 is 2·6% for the Nezbeda EOS, 4·40% for the EOS of Song and Mason and 7·3% for the Parsons equation. Although not presented in tables 13–16 we also considered the EOS of Boublík [21] and the average deviation was found to be slightly higher than that of Nezbeda. It is thus clear that from all the analytical EOSs considered in this work the EOS of Nezbeda gives the best results for hard ellipsoids. It should be noted that the EOS of Nezbeda [20] was

Table 13. EOS for hard ellipsoids with c = 3 and different values of b as obtained from MC and from several theoretical treatments. Results from simulation are labelled as Z_{MC}, results from equation (20) are Z_{new}, from the EOS of Nezbeda (equation (15)) are Z_{Nezbeda}, from the EOS of Song and Mason (equation (16)) are Z_{SM} and from the EOS of Parsons (equation (17)) as Z_{Parsons}. The value of Δ as defined in equation (19) of the text is presented in the last row.

b	ρ^*	Z_{MC}	Z_{new}	Z_{Parsons}	Z_{SM}	Z_{Nezbeda}
1	0·352	2·84	2·77	2·68	2·80	2·79
1	0·568	5·28	5·21	4·98	5·34	5·29
1	0·721	8·32	8·29	7·92	8·51	8·44
1	0·869	13·81	13·37	12·84	13·63	13·55
1·7320	0·365	2·74	2·74	2·65	2·75	2·74
1·7320	0·583	5·15	5·16	4·90	5·18	5·15
1·7320	0·730	8·22	8·08	7·64	8·09	8·05
1·7320	0·891	13·47	13·60	12·92	13·59	13·55
3	0·382	3·10	3·09	2·92	3·06	3·04
3	0·573	5·55	5·51	5·06	5·42	5·37
3	0·764	10·03	10·00	9·08	9·74	9·66
3	0·859	13·57	13·67	12·43	13·22	13·14
Δ			1·02	6·24	1·55	1·66

Table 14. EOS for hard ellipsoids with c = 4 and different values of b as obtained from MC and from several theoretical treatments. Rest of the notation as in table 13.

b	ρ^*	Z_{MC}	Z_{new}	Z_{Parsons}	Z_{SM}	Z_{Nezbeda}
1	0·331	3·02	2·94	2·82	3·02	2·97
1	0·540	5·56	5·55	5·26	5·85	5·70
1	0·685	8·76	8·65	8·23	9·16	8·91
1	0·754	10·61	10·73	10·26	11·33	11·03
2	0·354	2·82	2·94	2·80	2·96	2·93
2	0·553	5·42	5·37	4·99	5·42	5·34
2	0·698	8·60	8·39	7·76	8·44	8·33
2	0·767	10·43	10·43	9·66	10·47	10·33
4	0·331	3·02	3·07	2·81	3·02	2·97
4	0·528	5·68	5·79	5·07	5·64	5·50
4	0·682	8·80	9·41	8·15	9·08	8·53
4	0·753	10·62	11·79	10·22	11·30	11·00
Δ			2·9	6·3	2·8	2·6

Table 15. EOS for hard ellipsoids with $c = 5$ and different values of b as obtained from MC and from several theoretical treatments. Rest of the notation as in table 13.

b	ρ^*	Z_{MC}	Z_{new}	$Z_{Parsons}$	Z_{SM}	$Z_{Nezbeda}$
1	0·320	3·12	3·16	3·01	3·32	3·22
1	0·437	4·58	4·60	4·34	4·94	4·74
1	0·515	5·83	5·86	5·52	6·37	6·07
1	0·573	6·98	7·00	6·62	7·66	7·27
2·2361	0·337	2·96	3·07	2·88	3·10	3·05
2·2361	0·450	4·45	4·38	4·04	4·45	4·35
2·2361	0·533	5·63	5·66	5·18	5·77	5·62
2·2361	0·588	6·80	6·70	6·13	6·85	6·66
5	0·307	3·26	3·21	2·89	3·18	3·08
5	0·426	4·69	4·84	4·19	4·77	4·57
5	0·501	5·99	6·18	5·29	6·09	5·81
5	0·559	7·16	7·44	6·33	7·33	6·96
Δ			1·8	7·9	4·1	3·0

Table 16. EOS for hard ellipsoids with $c = 10$ and different values of b as obtained from MC results of [16] and from several theoretical treatments. Rest of the notation as in table 13.

b	ρ^*	Z_{MC}	Z_{new}	$Z_{Parsons}$	Z_{SM}	$Z_{Nezbeda}$
1	0·106	1·90	1·90	1·85	1·98	1·92
1	0·212	3·20	3·18	2·97	3·53	3·25
1	0·283	4·44	4·33	3·93	4·95	4·40
3·1623	0·283	3·69	3·67	3·29	3·86	3·60
3·1623	0·354	4·70	4·73	4·21	5·11	4·68
3·1623	0·424	5·78	5·96	5·34	6·64	5·99
3·1623	0·495	6·97	7·38	6·74	8·51	7·55
10	0·106	2·00	2·01	1·84	1·98	1·92
10	0·212	3·46	3·61	2·97	3·53	3·25
10	0·283	4·50	4·94	3·925	4·95	4·40
Δ			2·8	8·8	8·9	3·1

obtained by analysing the first virial coefficients of prolate spherocylinders only. It can be used with quite good results for prolate spheroids. This can be understood on the basis that virial coefficients of prolate convex bodies (spheroids or spherocylinders) fall almost on the same curve when plotted as a function of α, as noted by several authors [6, 43, 44]. The success of the EOS of Nezbeda is due to the fact that it is a good EOS for prolate convex bodies (it was designed for that purpose). Moreover, since this EOS depends on α only, it predicts prolate–oblate symmetry. We have already discussed that the EOS of prolate and oblate spheroids, although not identical are quite similar. Because of that, Nezbeda's EOS does a good job. The Song and Mason EOS works reasonably well, although it is inferior to the EOS of Nezbeda. Finally, Parsons EOS, although quite popular in theoretical studies is clearly inferior to the other two. However, the three EOS considered in this work, although relatively accurate, are not quite satisfactory in two fundamental points. (i) They predict prolate–oblate symmetry. Although prolate and oblate spheroids present a similar EOS it should not be forgotten that the EOS is not identical for these two types of molecules. (ii) Although the second virial coefficient is correctly predicted by these three EOS, predictions for the third, fourth and fifth virial coefficients are not so good. In fact, in figures 2, 3 and 4 the third, fourth and fifth virial coefficients of hard ellipsoids with $c = 10$ predicted by the EOS of Nezbeda and that of Song and Mason are compared to the numerical results of this work. As can be seen, for these rather anisotropic models, the predictions from these EOS are rather poor. These EOSs predict prolate–oblate symmetry in the third, fourth and fifth virial coefficients and this symmetry is not present in the computed virial coefficients. As was mentioned in section 3, it is not possible to describe the virial coefficients of hard ellipsoids with only a non-sphericity parameter. This is the reason of the failure of the Nezbeda and Song and Mason equations of state concerning predictions of virial coefficient for very anisotropic molecules of general shape (prolate uniaxial, biaxial, oblate uniaxial). In the light of the poor predictions of virial coefficients of the EOS of Nezbeda and Song and Mason it is rather surprising that these EOSs work so well (see table 16). Certainly, there is some cancellation of errors, so that some virial coefficients are underestimated and others are overestimated. The prediction of virial coefficients is especially important for very anisotropic molecules. In fact, for quite anisotropic molecules the range of densities where the isotropic phase is stable shrinks considerably, and therefore a good prediction of the virial coefficients is crucial.

Therefore there is room for improvement and the search of an EOS for hard ellipsoids should not be forgotten. In this work we have evaluated the first five virial coefficients of a number of hard ellipsoids. One question which naturally arises is the following: can the information provided by the virial coefficients be used to provide a reasonably good EOS? The first obvious approach is to use the virial expansion using the virial coefficients up to the fifth. While this is satisfactory for very elongated ellipsoids it is not a good approach when the ellipsoids are of moderate anisotropy, since the contribution of higher virial coefficients is important in this case. Therefore, the contribution of virial coefficients higher than the sixth should be included especially at moderate anisotropies. In Parsons' [22] EOS, all virial coefficients of the hard non-spherical particle are approximated by those of hard spheres multiplied by the ratio between the second virial coefficient of the hard non-spherical particle and that of a hard sphere. Since Parsons'

approach gives reasonable results for the EOS of hard ellipsoids, we decided to use this approach for including the contribution of virial coefficients higher than the fifth. Therefore the EOS proposed in this work for hard ellipsoids is given by:

$$Z = 1 + B_2^* y + B_3^* y^2 + B_4^* y^3 + B_5^* y^4 + \frac{B_2}{4}\left(\frac{1 + y + y^2 - y^3}{(1 - y)^3} - 1 - 4y - 10y^2 - 18{\cdot}3648y^3 - 28{\cdot}2245y^4 \right). \quad (20)$$

The origin of this equation is simple. We use the virial coefficients up to the fifth as determined numerically in this work. Higher virial coefficients are included following Parsons' prescription by a simple scaling of those of hard spheres. Contribution of virial coefficients higher than the fifth to the compressibility of hard spheres are obtained by subtracting from the Carnahan–Starling equation the contribution of the first five virial coefficients. The predictions obtained by this new EOS are presented in tables 13–16. As can be seen the agreement is good. In fact, the overall error obtained by this new EOS is 2·1%. The overall error obtained with Nezbeda EOS is 2·6%. Therefore the new proposed EOS may be considered as an improvement at least for hard ellipsoids over previously proposed EOSs. We should note that the improvement is rather modest. In that respect the equations of state of Nezbeda and of Song and Mason perform surprisingly well, especially taking into account that their predictions of virial coefficients are rather poor. Certainly, some cancellation of errors occur in these equations, so that although they fail in the prediction of certain virial coefficients, this failure is compensated by other virial coefficients. The equation of state proposed here indicates the advantage of giving results comparable to those of the other equations, but giving correct values for the first five virial coefficients.

Another advantage of equation (20) is that it distinguishes between prolate and oblate spheroids. In fact, as can be seen from the results of tables 13–16, the new EOS correctly predicts higher values of the compressibility factor for oblate spheroids than for prolate ones. In fact, equation (20) correctly predicts that for a given volume fraction the compressibility factor increases from the invariant ellipsoid to the prolate spheroid, and from the prolate to the oblate one. Therefore, not only the average error is quite small, but also differences in the compressibility factor are predicted correctly.

We have applied equation (20) to other convex bodies such as prolate and oblate hard spherocylinders. In table 17, the results are presented. It can be seen that equation (20) works remarkably well also for hard spherocylinders. Therefore, equation (20) can be used with confidence for convex bodies, such as prolate spheroids or spherocylinders, oblate spheroids or spherocylinders and biaxial particles such as ellipsoids or spheroplatelets. We tested also equation (20) for non-convex bodies as rigid linear chains of tangent hard spheres for which the first virial coefficients are known [44]. However, the results were not so good as for convex bodies. It begins to be clear from the work of several authors that Parsons' approach works well for convex bodies and poorly for non-convex bodies [45]. For non-convex bodies new methods to estimate virial coefficients and equation of state should be developed as for instance that presented in [46]. In passing let us mention that the procedure proposed in [44] to build an EOS from the virial coefficients was also tested. It yields good results for prolate and oblate spheroids. However, since a different prescription is used for prolate and oblate molecules we did not found a trivial way of implementing the procedure for biaxial particles.

Table 17. EOS for hard spherocylinders as obtained from equation (20) and from the computer simulation results reported in [37]. Simulation results for the prolate spherocylinder with $L^* = 5$ were taken from [47]. Virial coefficients of hard spherocylinders were estimated by using equations (10)–(12).

L^*	y	Z_{MC}	Z_{new}
Prolate			
0·6	0·2948	4·10	4·13
0·6	0·3873	6·84	6·89
1	0·30	4·48	4·54
1	0·5096	16·80	16·22
2	0·30	5·40	5·34
2	0·50	18·00	18·19
5	0·09	2·01	2·02
5	0·31	8·16	8·16
5	0·352	10·31	10·47
Oblate			
1	0·25	3·35	3·34
1	0·45	10·56	10·48
2	0·25	3·83	3·82
2	0·45	12·30	12·44

An important objection to equation (20) is that it requires a knowledge of the first five virial coefficients which in general are not available. Therefore, it seems of limited applicability. However we have shown in section 3 that virial coefficients of hard ellipsoids can be obtained quite accurately from the empirical expressions given by equations (10)–(12) so that this objection can be countered. Moreover, equations (10)–(12) are useful for estimating the virial coefficients of a number of

convex bodies and they guarantee the applicability of equation (20).

6. Conclusions

In this work, the first five virial coefficients of hard ellipsoids with c in the range 3 to 10 have been computed numerically. Differences between prolate, invariant and oblate molecules were found in the third, fourth and fifth virial coefficients. It has been shown that the virial coefficients of hard ellipsoids can be correlated by an empirical expression which uses two non-sphericity parameters, namely, α and τ. Moreover, this expression describes successfully the virial coefficients of other convex bodies as, for instance, hard spherocylinders. The virial coefficients data provided in this work may be useful for checking new equations of state.

Computer simulations in the *NPT* ensemble were also performed. For a given length to breadth ratio and volume fraction the compressibility factor increases from the invariant ellipsoid to the prolate spheroid, and from the prolate spheroid to the oblate one. However, differences were found to be small, especially taking into account the large difference in virial coefficients between these models. The explanation is found in the fact that the joint contribution of the fourth and fifth virial coefficients is approximately equal for prolate and oblate molecules for a density not too far from the density at which the nematic phase appears.

Several analytical equations of state for hard convex bodies have been tested. It is found that for the ellipsoids considered in this work, the equation of state proposed by Nezbeda [20] yields the best agreement with simulation, followed by that proposed by Song and Mason. Parsons' scaling yields worse results than the other two equations of state. However, there is room for improvement. These three equations of state proposed predict prolate–oblate symmetry. This is a good approximation, but it is not exact. Moreover, the virial coefficients predicted by these EOSs are rather poor for the elongated ellipsoids considered in this work. We propose a new equation of state for hard ellipsoids which uses the computed virial coefficients. Basically, this equation is a truncated virial expansion, which uses Parsons' scaling to estimate the higher virial coefficients. Good agreement with simulation is found with this new equation of state. Although the improvement of the new EOS over that of Nezbeda is rather modest, the new EOS presents two important advantages. The first is that the new EOS breaks the prolate–oblate symmetry. Prolate and oblate spheroids according to this equation have a similar but not identical equation of state. The second is that this new EOS uses exact values for the first five virial coefficients. This is important for very anisotropic models, since for this type of molecule, the range of densities where the isotropic phase is stable becomes vanishingly small. The new EOS has been also applied to hard spherocylinders and again good agreement with simulation was found.

Dr J. L. F. Abascal is thanked for providing a code to perform the fitting described in section 3 of this work. This project has been financially supported by project PB94-0285 of the Spanish DGICYT (Dirección General de Investigación Científica y Técnica).

References

[1] Gray, C. G., and Gubbins, K. E., 1984, *Theory of Molecular Fluids* (Oxford, U.K.: Clarendon).
[2] Hansen, J. P., and McDonald, I. R., 1986, *Theory of Simple Liquids*, 2nd edition (New York: Academic Press).
[3] Onsager, L., 1949, *Ann. New York Acad. Sci.*, **51,** 627.
[4] Vieillard-Baron, J., 1972, *J. chem. Phys.*, **56,** 4729.
[5] Frenkel, D., and Mulder, B., 1985, *Molec. Phys.*, **55,** 1171.
[6] Rigby, M., 1989, *Molec. Phys.*, **66,** 1261.
[7] Lee, S. D., 1988, *J. chem. Phys.*, **89,** 7036.
[8] Tjipto-Margo, B., and Evans, G. T., 1990, *J. chem. Phys.*, **93,** 4254.
[9] Colot, J. L., Wu, X. G., Xu, H., and Baus, M., 1988, *Phys. Rev.* A, **38,** 2022.
[10] Vega, C., and Lago, S., 1994, *J. chem. Phys.*, **100,** 6727.
[11] Vroege, G. J., and Lekkerkerker, H. N. W., 1992, *Rep. Prog. Phys.*, **55,** 1241.
[12] Gelbart, W. M., 1982, *J. phys. Chem.*, **86,** 4296.
[13] Somoza, A. M., and Tarazona, P., 1992, *Molec. Phys.*, **75,** 17.
[14] Straley, J. P., 1974, *Phys. Rev.* A, **10,** 1881.
[15] Mulder, B. M., 1986, *Liq. Cryst.*, **1,** 539.
[16] Allen, M. P., 1990, *Liq. Cryst.*, **8,** 499.
[17] de Gennes, P. G., and Prost, J., 1993, *The Physics of Liquid Crystals* (Oxford: Clarendon Press).
[18] Isihara, A., 1951, *J. chem. Phys.*, **19,** 397.
[19] Singh, G. S., and Kumar, B., 1996, *J. chem. Phys.*, **105,** 2429.
[20] Nezbeda, I., 1976, *Chem. Phys. Lett.*, **41,** 55.
[21] Boublík, T., 1981, *Molec. Phys.*, **42,** 209.
[22] Parsons, J. D., 1979, *Phys. Rev.* A, **19,** 1225.
[23] Song, Y., and Mason, E. A., 1990, *Phys. Rev.* A, **41,** 3121.
[24] Ree, F. H., and Hoover, W. G., 1964, *J. chem. Phys.*, **40,** 939.
[25] Rigby, M., 1970, *J. chem. Phys.*, **53,** 1021.
[26] Allen, M. P., Evans, G. T., Frenkel, D., and Mulder, B., 1993, *Adv. chem. Phys.*, **86,** 1.
[27] Perram, J. W., and Wertheim, M. S., 1985, *J. comput. Phys.*, **58,** 409.
[28] Wood, W. W., 1970, *J. chem. Phys.*, **52,** 729.
[29] Allen, M. P., and Tildesley, D. J., 1987, *Computer Simulation of Liquids* (Oxford: Clarendon Press).
[30] Monson, P. A., and Rigby, M., 1978, *Molec. Phys.*, **35,** 1337.
[31] Wojcik, M., and Gubbins, K. E., 1984, *Molec. Phys.*, **53,** 397.
[32] Wertheim, M. S., 1996, *Molec. Phys.*, **89,** 1005.
[33] Kihara, T., 1963, *Adv. Chem. Phys.*, **5,** 147.

[34] HADWIGER, H., 1955, *Altes und Neues über konvexe Korper* (Basel: Birkhäuser).
[35] DIAZ PEÑA, M., RUBIO, R. G. and PEDRAZUELA, J., 1989, *Fluid Phase Equilibria*, **48,** 31.
[36] NAUMANN, K. H., and LELAND, T. W., 1984, *Fluid Phase Equilibria*, **18,** 1.
[37] BOUBLÍK, T., and NEZBEDA, I., 1986, *Collec. Czech. Chem. Commun.*, **51,** 2301.
[38] FRENKEL, D., 1988, *P. phys. Chem.*, **92,** 5314.
[39] COONEY, W. R., THOMPSON, S. M., and GUBBINS, K. E., 1989, *Molec. Phys.*, **66,** 1269.
[40] NEZBEDA, I., and BOUBLÍK, T., 1984, *Molec. Phys.*, **51,** 1443.
[41] SAMBORSKI, A., EVANS, G. T., MASON, C. P., and ALLEN, M. P., 1994, *Molec. Phys.*, **81,** 263.
[42] CARNAHAN, N. F., and STARLING, K. E., 1969, *J. chem. Phys.*, **51,** 635.
[43] RIGBY, M., 1989, *Molec. Phys.*, **68,** 687.
[44] VEGA, C., GARZON, B., and LAGO, S., 1994, *Molec. Phys.*, **83,** 1233.
[45] WILLIAMSON, D. C., 1995, *Phys.* A, **220,** 139.
[46] MAESO, M. J., and SOLANA, J. R., 1996, *Molec. Phys.*, **89,** 1209.
[47] MCGROTHER, S. C., WILLIAMSON, D. C., and JACKSON, G., 1996, *J. chem. Phys.*, **104,** 6755.